J. Appl. Comput. Mech., 6(2) (2020) 209-218
DOI: 10.22055/jacm.2019.28936.1521

ISSN: 2383-4536
jacm.scu.ac.ir

M&MoCS
Shahid Chamran University of Ahvaz

Journal of
Applied and Computational Mechanics

Research Paper

Effect of Corrugated Baffles on the Flow and Thermal Fields in a Channel Heat Exchanger

Houari Ameur

Department of Technology, University Centre of Naama - Ahmed Salhi (Ctr Univ Naama)
Po. Box 66, 45000, Algeria, E-mail: houari_ameur@yahoo.fr

Received March 16 2019; Revised May 28 2019; Accepted for publication June 22 2019.
Corresponding author: Houari Ameur (houari_ameur@yahoo.fr)

Abstract. The performance of corrugated baffles inserted in a rectangular channel heat exchanger is investigated. The fluid flows and thermal distribution are determined via numerical simulations. The working fluid has a shear thinning behavior. The influence of the baffle design is explored, we interest to the "wavy" shape. The corrugation angle of baffle (α) is changed from 0° (i.e. a straight baffle) to 45°. Also, the height (h) of the corrugated baffle is changed and three cases are considered, namely: h/H = 0.4, 0.5 and 0.6, where "H" is the channel height. In comparison with the unbaffled channel, the overall performance factor has increased from 1.27 up to 1.53 when the corrugation angle is increased from 0° to 45°. Concerning the corrugation height, the predicted results allowed us to select the case h/H = 0.5 as the best configuration from the cases studied.

Keywords: Heat exchanger; Corrugated baffles; Baffle design; Laminar flow; Non-Newtonian fluids.

1. Introduction

Different techniques are used to enhance heat transfer such as fin, jet impinging and modification of wall surfaces by introducing various protrusions. The vortex generators are well-known for their efficiency in heat transfer enhancement [1-7]. They are encountered in various engineering applications such as heat exchanger, vortex combustor, gas turbine, drying process, biodiesel, etc. [8, 9].

Many studies have been achieved for different shapes of vortex generators, such as angled baffles [10, 11], V-shaped baffles [12], W-shaped baffles [13], inclined V-shaped discrete thin baffles [14], arc-shaped baffles [15], orthogonal baffles [16], diamond-shaped baffles [17], isosceles triangular baffles [18], Z-shaped baffles [19] and other different shaped baffles [20-22].

The presence of baffles in a channel heat exchanger interrupt the hydrodynamic and thermal boundary layers, leading thus in augmented heat transfer rates. Many researchers focused on the effect of baffles and their shape and arrangement. Compared to the smooth channel, Sahu and Bhagoria [23] found an enhancement in heat transfer by about 1.25-1.4 times with a rectangular channel roughened by broken transverse baffles. Aharwal et al. [24] conducted an experimental investigation on the performance of inclined square split-baffle with a gap on one wall of a rectangular channel and they found an augmentation in friction factor and Nusselt number by about 2.3 to 2.9 and 1.5 up to 2.6 times higher than those for the smooth channel, respectively. The increase of blockage ratio of baffles participates in the increase of Nusselt number, as reported by Taslim et al. [25]. Due to the breaking of laminar sub-layer and formation of secondary flows, the inclined baffle yields higher heat transfer rates than that of the transverse baffle. And due to reduced force drag, the reduced attack angle decreases the friction factor [26]. For a rectangular channel, the increase in the number of baffled walls yields a rise in heat transfer rates, as reported by Chandra et al. [27]. The experimental works

Published online: August 28 2019

achieved by Promvonge et al. [28, 29] on the turbulent flow over 30° angle–finned tapes fitted diagonally in a rectangular channel revealed that the smaller fin pitch spacing yields the highest heat transfer and pressure drop. For a rectangular heat exchanger channel, Yang et al. [30] pointed out that the staggered arrangement baffles give less high heat transfer coefficient than the symmetric arrangement baffles. Also, the one-side baffled channel provides less heat transfer rates than the two-side baffled one. Ke et al. [31] investigated by numerical simulations the performance of delta-shaped winglet longitudinal vortex generators (LVGs) in a rectangular channel. Their results revealed that the LVG aspect ratio and channel height are the two most critical factors influencing the performance of this kind of LVGs. For solar air heater and *Re* ranging between 3000 and 15,000, Singh et al. [26] compared the performance of transverse baffles having a uniform cross-section (trapezoidal, square and circular) with other baffles having a non-uniform cross-section in the form of saw-tooth. The maximum enhancement in Nusselt number was obtained with the saw-tooth baffles, followed by the trapezoidal form (1.78 and 1.50, respectively). The saw-tooth baffles have given the lowest value of friction factor (a maximum enhancement in f by 2.49).

For the corrugated shape of baffles, only a few papers are available in the literature. Menni et al. [32] studied the turbulent forced convection in a channel provided by staggered corrugated baffles. Benzenine et al. [33] studied by numerical simulation the turbulent air flow in a rectangular channel equipped with two waved baffles sequentially arranged in the bottom and top of the channel walls. They used plane and waved baffles at different inclination angles (0° up to 45°). They found an improvement in the skin friction by about 9.91% in the case of undulated baffle inclined by 15°, and improvement in pressure drop starter from 10.43% in all cases compared with the plane baffles. For a solar air collector, Kumar and Chand [34] studied the performance of herringbone corrugated fins inserted below the absorber plate along the fluid flow channel. Compared to the conventional solar air heater and for a fixed mass flow rate of 0.026 kg/s, they found an improvement from 36.2% to 56.6% with fin pitch 2.5 cm.

As exhibited in the previous literature review, the case of non-Newtonian fluid flows through heat exchangers with corrugated baffles seems to be not treated. Therefore, the purpose of this work is to investigate the development of flow and thermal fields of the most common class of non-Newtonian fluids, the shear-thinning fluids, in a heat exchanger equipped with corrugated baffles. Effects of some geometric parameters on convection and pressure drop are highlighted. It concerns the waviness angle of baffles and their height.

As known, the design of heat exchangers is not an easy task when complex non-Newtonian fluids are involved. This issue concerns primarily chemical and food industries wherein products to be treated may exhibit complex rheological behavior. Also, such fluids as fruit purees and tomato sauces have generally high apparent viscosity, so the cooling inside the exchanger exhibits a complexity [35].

2. Problem Studied

The geometry of the problem studied is shown in Fig. 1. It concerns a rectangular channel having baffles on the upper and lower walls. All required details on geometric parameters are provided in Table 1 and Fig. 1.
The fluid used is the Ketrol solution which has the following rheological properties: consistency index k = 9.5 Pa s^n, power law index n = 0.8 and density ρ = 997 kg/m^3. The inlet temperature of hot fluid is 333 K and the temperature at the upper and lower walls of the channel is 268 K. The left and right surfaces of channel are supposed to be symmetric.
Effects of the corrugation angle (α) are explored via the creation of three geometries, which are α = 0°, 22.5° and 45°. Also, effect of the baffle height (h) is investigated by realizing three geometrical configurations, namely: h/a = 0.4, 0.5 and 0.6.

Table 1. Details on geometric parameters of the problem studied

L [mm]	H/L	l/L	h/L	W/L	w/L
400	0.05	0.156	0.025	0.156	0.005

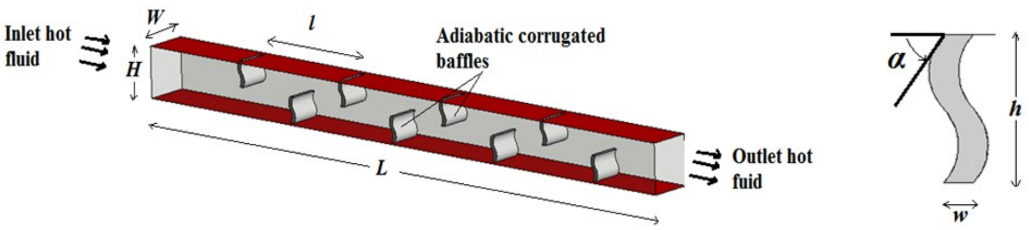

Fig. 1. Geometry of the problem studied

3. Governing Equations

The behavior of the fluid flowing through the channel is shear-thinning, which is modeled by the Ostwald law. The shear stress and apparent viscosity are determined by Eqs. (1) and (2) as follows:

$$\tau = k\dot{\gamma}^{n} \tag{1}$$

$$\eta = k\dot{\gamma}^{n-1} \tag{2}$$

where τ is the shear stress, $\dot{\gamma}$ is the shear rate and η is the apparent viscosity.

The flow is continuous and steady-state and the heat transfer is natural. Also, the flow laminar where Reynolds number for a shear-thinning fluid is given by:

$$Re = \frac{\rho\, U^{2-n}\, D_h^n}{m}\left(\frac{3n+1}{4n}\right)^{-n} 8^{1-n} \tag{3}$$

where D_h is the hydraulic diameter.

$$D_h = \frac{4\,LA_c}{A_t} \tag{4}$$

where A_c is the minimum cross sectional flow area. The continuity, momentum and energy equations are given as:

- Conservation of continuity:

$$\frac{\partial}{\partial x_i}(\rho u_i) = 0 \tag{5}$$

- Conservation of momentum:

$$\frac{\partial}{\partial x_i}(\rho u_i u_k) = \frac{\partial}{\partial x_i}\left(\mu_a \frac{\partial u_k}{\partial x_i}\right) - \frac{\partial p}{\partial x_k} \tag{6}$$

- Conservation of energy:

$$\frac{\partial}{\partial x_i}(\rho u_i T) = \frac{\partial}{\partial x_i}\left(\frac{k_f}{C_p}\frac{\partial T}{\partial x_i}\right) \tag{7}$$

where C_p is the specific heat of working fluids. The heat transfer coefficient and pressure drop are usually expressed in terms of dimensionless factors. Two well-known dimensionless parameters, Colburn factor, j, and Fanning friction factor, f, were used to describe the heat transfer performance and pressure drop characteristics:

$$j = \frac{h}{\rho u C_p} Pr^{\frac{2}{3}} \tag{8}$$

$$f = \frac{2\Delta p}{\rho u^2}\frac{D_h}{L} \tag{9}$$

where Pr is the Prandtl number, D_h is the hydraulic diameter and h is the convective heat transfer coefficient, given by:

$$h = \frac{Q_{conv}}{A_t\,(T_w - T_b)_{LMTD}} \tag{10}$$

where A_t is the total heat transfer area and Q_{conv} is the convective heat transfer rate expressed as follows:

$$Q_{conv} = mC_p\left(T_{b,out} - T_{b,in}\right) \tag{11}$$

where m is the mass flow rate, $T_{b,in}$ and $T_{b,out}$ are the average temperature of fluid at the inlet and outlet of test section, respectively. $(T_w - T_b)_{LMTD}$ is the log mean temperature difference given by:

$$(T_w - T_b)_{LMTD} = \frac{\Delta T_{w\text{-}b,in} - \Delta T_{w\text{-}b,out}}{\log\left(\dfrac{\Delta T_{w\text{-}b,in}}{\Delta T_{w\text{-}b,out}}\right)} \tag{12}$$

where $\Delta T_{w\text{-}b,in}$ and $\Delta T_{w\text{-}b,out}$ denote the differences between the wall temperature and the bulk fluid temperature at the inlet and outlet of heat transfer section. The Δp is the pressure difference between inlet and outlet defined as:

$$\Delta p = p_{av,in} - p_{av,out} \tag{13}$$

where subscripts 'av, in' and 'av, out' refer to the average pressure values at the inlet and outlet cross sections.

4. Numerical Details

The geometry of the problem studied is created by the computer tool ICEM CFD and the computational domain is meshed by tetrahedral grid elements (Fig. 2). A control volume approach is used for the discretization of the governing equations. Also, a refined mesh near the heat exchanger walls was created in order to capture details of the hydrodynamic and thermal boundary limit. Many cases of unstructured meshes were created to ensure the accuracy and consistency of the predicted results. The non-uniform grid was confirmed to be efficient to have the independency of predicted results from the grid system. This was concluded by achieving grid independency tests (comparison of the pressure drop results and relevant errors for various grids). After mesh test, the selected mesh grid had about 1.2 million of elements.

For the boundary conditions, a uniform inlet velocity and a uniform inlet temperature T = 333 K and non-slip boundary condition for the fluid velocity at the walls are used. All axial derivatives are considered to be zero at the exit of the channel, i.e. the fully developed assumption is used. A fixed temperature T_w = 268 K is imposed at the upper and lower walls of the channel. The side surfaces of the channel were considered to be symmetric. Baffles are considered to be adiabatic. The constant intensity turbulence of 1% is employed. Further, the turbulent kinetic energy and its dissipation are equal to zero.

The computer code CFX (version 18.0) was used to conduct all computations. The SIMPLE (Semi Implicit Method for Pressure Linked Equation) algorithm was used to perform pressure-velocity coupling. The diffusion term was approximated in the momentum and energy equations by the second-order central difference. For the discretization of convection terms, a second-order upwind scheme was adopted. The above mentioned governing equations were solved by a segregated implicit iterative scheme. To ensure the computational convergence, the following under-relaxation factors were set for the pressure, momentum and energy, respectively: 0.3, 0.7, and 0.8. The residual target was set to 10^{-7} for the continuity, momentum and energy equations. With a machine (Intel Core i7 CPU, 2.20 GHz of clock speed and 8.0 GB of RAM), the convergence took about 1300-1600 iterations and 5-6h of CPU time.

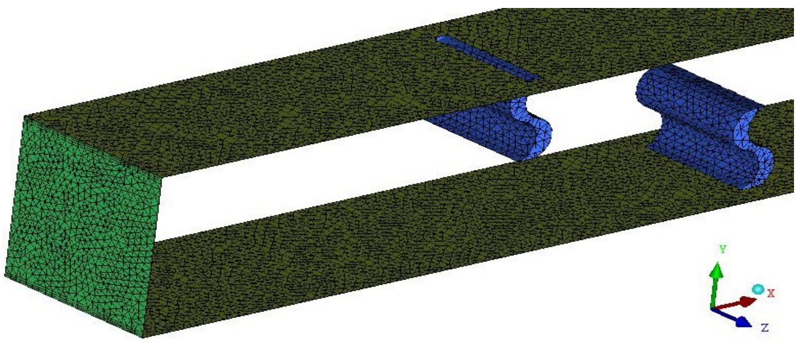

Fig. 2. Meshing of the computational domain with tetrahedral elements

5. Validation

In order to confirm the reliability of the calculation code and the accuracy of the numerical method undertaken, we proceed to the validation of some predicted results. For this purpose, we referred to the experimental work of Demartini et al. [36]. We note that the working fluid used by Demartini and his co-workers is Newtonian (air) and the baffles inserted in the channel are plane. Where the channel height is 0.167 m and the baffle height is 0.08 m, U_0 is the entrance velocity, 7.8 m/s, and the total length of the channel is equivalent to 3.307 hydraulical diameters. Our predicted results of the axial velocity along the channel height are presented in Fig. 3 and compared with the experimental data of Demartini et al. [36]. As observed, the validation shows a satisfactory agreement.

6. Results and Discussion

The insert of periodic baffles in the channel heat exchangers yields an interruption of thermal and hydrodynamic layers. The flow of fluid separates re-circulates and impinges on the walls of the channel after the passage of each baffle. The fluid flow is also altered by these vortex generators where their design and configuration should be optimized. These phenomena are the main reasons of the improvement of heat transfer. However, a substantial increase in pressure loss remains a major issue [37]. Until present, researchers continue in the development of various methods and techniques to respond to the industries needs of higher thermal performances.

6.1. Effect of the corrugation angle

The presence of baffles in heat exchangers is known as an efficient technique in terms of improving thermal performance. In the first part of our investigation, we look for the influence of the vortex generator design (VG) on the thermo-hydraulic performance. The exchanger studied is a horizontal and rectangular channel provided with vertical baffles. The baffles are supposed adiabatic while the wall has a fixed and low temperature. The objective of these baffles is to generate turbulence even at low Reynolds number and to increase the residence time of the hot fluid. This can serve as a heat exchange promoter, which will allow a reduction in the length traversed by the hot fluid before it will be cooled.

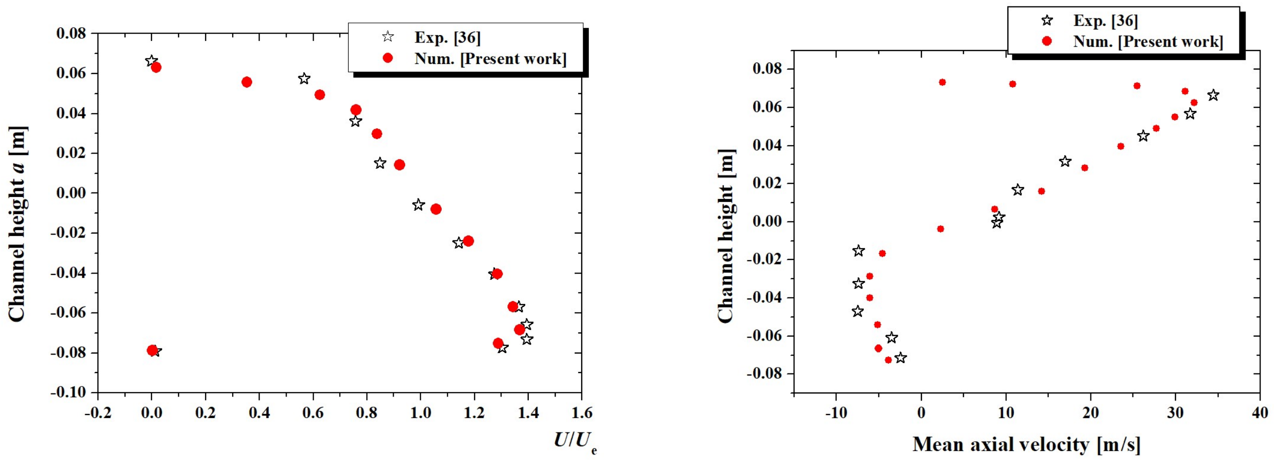

(a) (b)

Fig. 3. (a) Axial velocity versus the channel height upstream of the first baffle plate, Re = 200, x = 0.159, (b) Mean axial velocity after the second baffle plate, near the channel outlet, x = 0.525

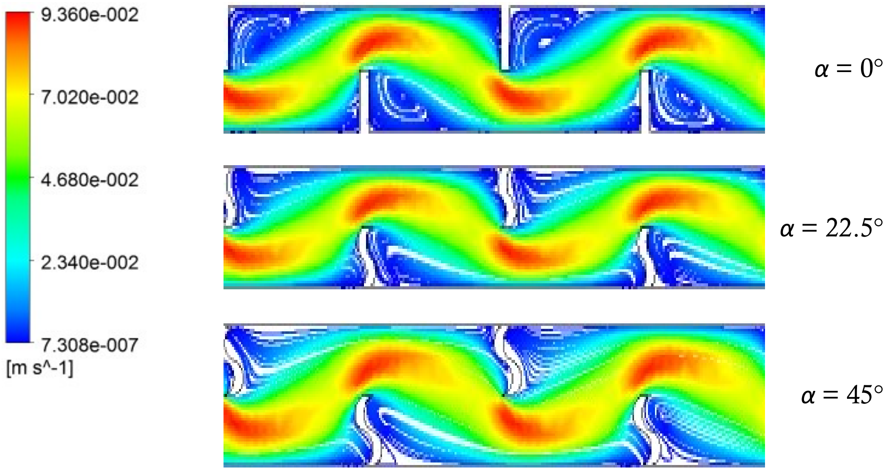

Fig. 4. Streamlines for Re = 30, $h/H = 0.5$

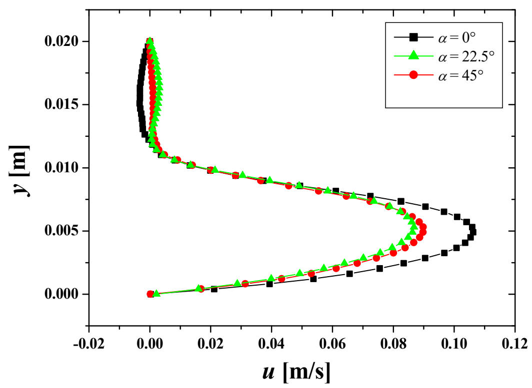

Fig. 5. Axial velocity behind the baffle, for Re = 30, h/H = 0.5

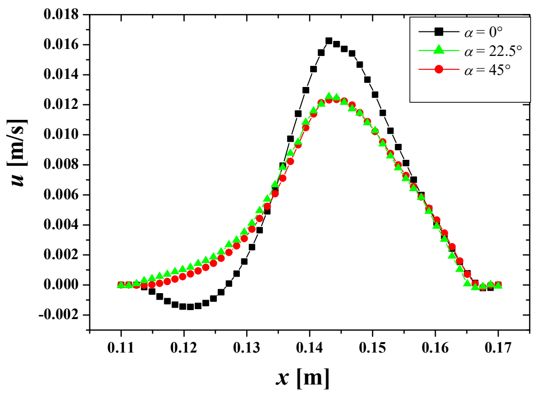

Fig. 6. Axial velocity near the channel wall, at the mid-distance between 2 baffles, Re = 30, $h/H = 0.5$

In this section, an investigation into the effects of baffle curvature is made. Three angles of curvature are considered which are: α = 0° (which corresponds to a straight baffle), α = 22.5° and α = 45°. Results of the velocity fields are shown in Fig. 4 for the three values of corrugations. The first observation to emphasize is the periodicity of the flow regardless of the curvature of the baffle. Also, the speed is the highest at the baffle tip, and it decreases gradually behind this VG and the flow is re-circulated in this region. The comparison between the three cases studied shows that the size of vortex developed behind the baffle is greater for $\alpha = 0°$, then it begins to decrease with the increase of α. In the case of $\alpha = 45°$, a secondary vortex is formed just after the baffle tip.

More explanation on the velocity distribution is shown in Figs. 5 and 6, where the axial velocity is followed vertically for a position just after the baffle, then horizontally over a distance between two consecutive baffles which correspond to a position very close to the wall, respectively. It is clear that the increase of corrugation angle decreases the intensity of the axial component of velocity (Fig. 5). The negative values of velocity (in Fig. 6) indicate the existence of recirculation of the flow. Then, for a position close to the wall, the main vortex appeared for a flat baffle, and then it will be dissipated by increasing the curvature of the baffle. The thermal fields for the three cases of corrugated baffles are shown in Fig. 7. Reducing the recirculation zone developed behind the baffle with the increase of α weakens the intensity of molecular interaction, and as a result, the cooling of the liquid will be less effective. But on the other hand, this can be useful in terms of reducing the pressure drop. This fall is mainly due here to the geometrical singularity (Fig. 8).

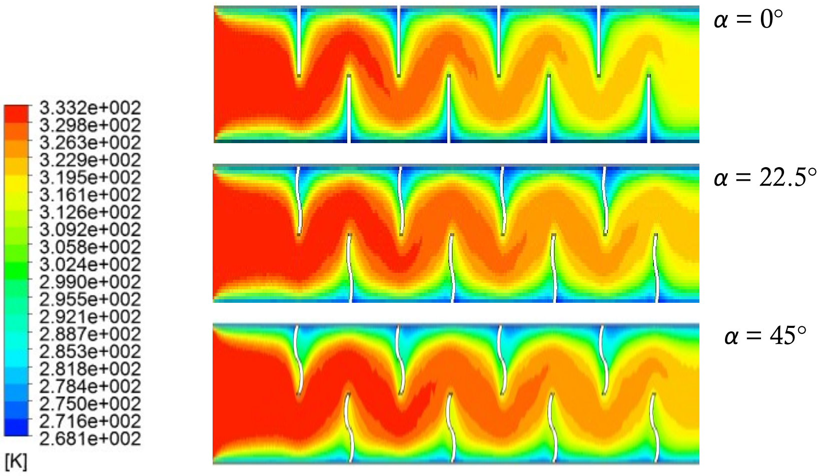

Fig. 7. Thermal fields for $Re = 5$, $h/H = 0.5$

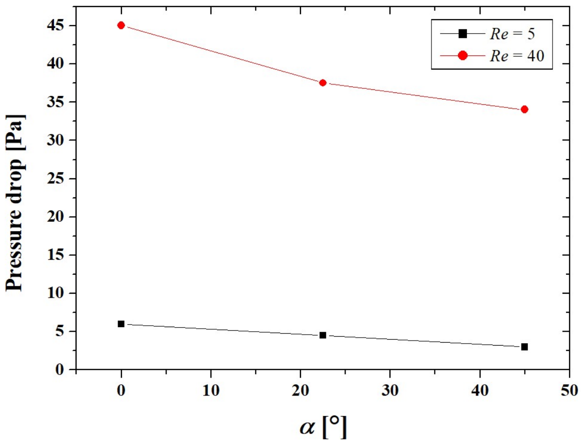

Fig. 8. Pressure drop for $h/H = 0.5$

Results of the overall thermal performance factor for different corrugation angles are presented in Fig. 9. We remind that this factor takes into account the friction factor and heat transfer coefficient, as defined by Eqs. (8) and (9). As shown in this figure, the performance factor is superior than 1 for all cases, which means that the baffling technique is an efficient technique to enhance the performance of such exchangers. Furthermore, the performance factors for the corrugation angles 0°, 22.5° and 45° are: 1.27, 1.40 and 1.53, respectively. We remind that these values are compared with the case of unbaffled channel and the case 0° corresponds to the plane baffle.

The undulation of baffle leads to a good enhancement of the overall performance factor. This is due to the curved shape which allows an easy passage of fluid particles around the baffle accompanied with a rotation of fluid, resulting thus in intensified interaction between fluids particles and reduced pressured drop.

6.2. Effect of the baffle height (*h*)

Effect of another geometrical parameter is analyzed in this section; it concerns the baffle height (h/H). Three geometric configurations were realized to carry out the test and which are: $h/H = 0.4$, 0.5 and 0.6.

The predicted results for temperature and pressure drop are shown in Figs 10 and 11, respectively. The baffle height has a major effect on the performance of the exchanger:

- Increasing the ratio h/H increases the residence time of the fluid, which reduces the distance traversed by the hot fluid.
- A second consequence is the considerable growth of pressure drops.

So this h/H ratio needs to be optimized. To our belief, this ratio must not exceed the ratio 0.5.

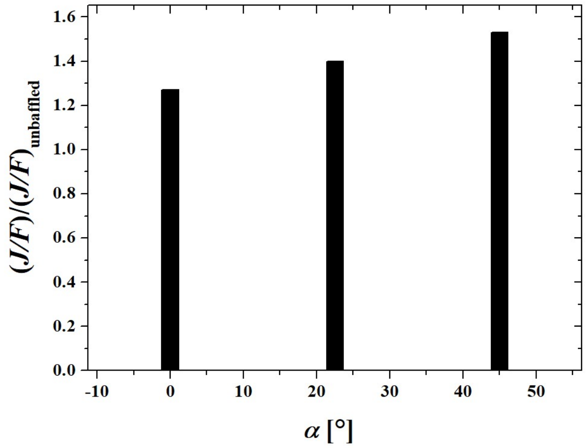

Fig. 9. Performance factor for $Re = 30$

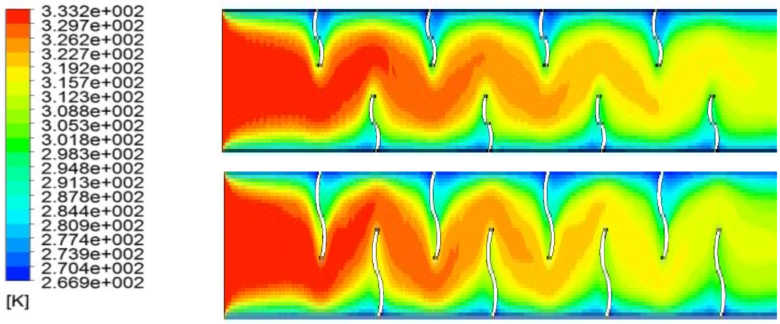

Fig. 10. Thermal fields for $Re = 3$, $\alpha = 22.5°$

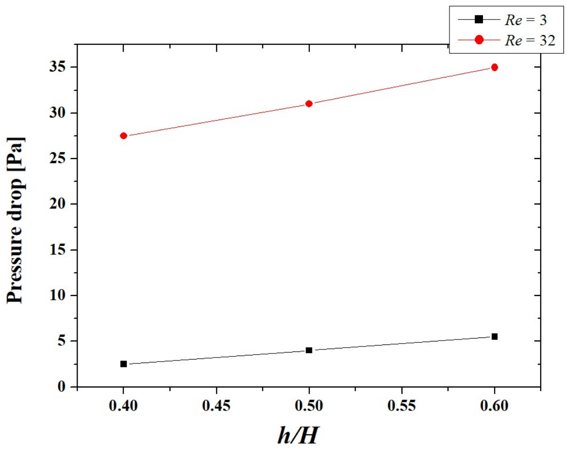

Fig. 11. Pressure drop for $\alpha = 22.5°$

7. Conclusion

The performance of a rectangular channel heat exchanger equipped with baffles was analyzed by numerical simulation. The calculation code used has allowed a three-dimensional visualization of thermal and hydrodynamic fields throughout the volume of the exchanger. Effects of the baffle shape have been explored; we have been interested in the "wavy" shape. The ripple angle (α) has been varied from 0° to 45°, where the value of 0° corresponds to a straight baffle. Also, effects of the height of the corrugated baffle were highlighted. The obtained results confirmed the need to optimize the design of such heat exchanger. The straight baffle has been found to be better than the corrugated baffle in terms of heat exchange intensification, since the vortex size region, in which there are strong molecular interactions, is wider. But, the maximum value of the pressure drop was observed for the design (α = 0 °). In comparison with the unbaffled channel, the performance factor has increased from 1.27 up to 1.53 when the corrugation angle is increased from 0° to 45°. Finally, concerning the baffle height which plays also a role in improving the thermal efficiency, the obtained results allowed us to qualify the case h/H = 0.5 as the best configuration.

Conflict of Interest

The author declared no potential conflicts of interest with respect to the research, authorship and publication of this article.

Funding

The author received no financial support for the research, authorship and publication of this article.

Nomenclature

a, H	Channel height	m
A_c	The minimum cross sectional flow area	m^2
A_t	Total surface area in contact with working fluid	m^2
h	height of baffle	m
W	Width of channel in z direction	m
w	Width of baffle	m
D_h	Hydraulic diameter, $D_h = (4\,L\,A_c)/(A_t)$	m
h	Effective heat transfer coefficient	W m^{-2} K^{-1}
k	Consistency index	Pa s^n
L	Length of channel	m
l	Distance between two consecutives ranges of baffles	m
m	Mass flow rate	Kg s^{-1}
n	Power law index	-
Δp	Pressure drop	Pa
Q_{conv}	Convective heat transfer rate	W
T	Temperature	K
T_{in}	Inlet temperature	K
T_w	Wall temperature	K
$T_{b,in}$, $T_{b,out}$	The average temperature of fluid at the inlet and outlet of test section	K
$(T_w - T_b)_{LMTD}$	log mean temperature difference	K
$\Delta T_{w\text{-}b,\,in}$	Differences between the wall temperature and the bulk fluid temperature at the inlet of heat transfer section	K
$\Delta T_{w\text{-}b,\,out}$	Differences between the wall temperature and the bulk fluid temperature at outlet of heat transfer section	K
u	Mean velocity	m s^{-1}

Greek symbols

σ	Corrugation angle of baffle	Degree
μ_a	Apparent viscosity	Pa s
ρ	Density	kg m^{-3}
$\dot{\gamma}$	Shear rate	s^{-1}
C_p	Specific heat	J kg^{-1} K^{-1}
k_f	Thermal conductivity	W m^{-1} K^{-1}

Dimensionless groups

f	Fanning friction factor
j	Colburn factor
Nu	Nusselt number
Pr	Prandtl number
Re	Reynolds number

References

[1] K. Alem, D. Sahel, A. Nemdili, H. Ameur, CFD investigations of thermal and dynamic behaviors in a tubular heat exchanger with butterfly baffles, *Frontiers Heat Mass Transfer* 10 (2018) 27.

[2] K. Boukhadia, H. Ameur, D. Sahel, M. Bozit, Effect of the perforation design on the fluid flow and heat transfer characteristics of a plate fin heat exchanger, *International Journal of Thermal Sciences* 126 (2018) 172-180.

[3] M. Mellal, R. Benzeguir, D. Sahel, H. Ameur. Hydro-thermal shell-side performance evaluation of a shell and tube heat exchanger under different baffle arrangement and orientation, *International Journal of Thermal Sciences* 121 (2017) 138-149.

[4] D. Sahel, H. Ameur, R. Benzeguir, Y. Kamla. Enhancement of heat transfer in a rectangular channel with perforated baffles, *Applied Thermal Engineering* 101 (2016) 156-164.

[5] D. Sahel, H. Ameur, Y. Kamla. A numerical study of fluid flow and heat transfer over a fin and flat tube heat exchangers with complex vortex generators, *European Physical Journal Applied Physics* 78 (2017) 34805.

[6] G. Liang, M.D. Islam, N. Kharoua, R. Simmons, Numerical study of heat transfer and flow behavior in a circular tube fitted with varying arrays of winglet vortex generators, *International Journal of Thermal Sciences* 134 (2018) 54-65.

[7] Y. Lei, F. Zheng, C. Song, Y. Lyu, Improving the thermal hydraulic performance of a circular tube by using punched delta-winglet vortex generators, *International Journal of Heat and Mass Transfer* 111 (2017) 299-311.

[8] E. Jiaqiang, D. Han, Y. Deng, W. Zuo, C. Qian, G. Wu, Q. Peng, Z. Zhang, Performance enhancement of a baffle-cut heat exchanger of exhaust gas recirculation, *Applied Thermal Engineering* 134 (2018) 86-94.

[9] E. Jiaqiang, M. Yue, J. Chen, H. Zhu, Y. Deng, Y. Zhu, F. Zhang, M. Wen, B. Zhang, S. Kang, Effects of the different air cooling strategies on cooling performance of a lithium-ion battery module with baffle, *Applied Thermal Engineering* 144 (2018) 231-241.

[10] M.S. Lee, S.S. Jeong, S.W. Ahn, J.C. Han, Effects of angled ribs on turbulent heat transfer and friction factors in a rectangular divergent channel, *International Journal of Thermal Sciences* 84 (2014) 1-8.

[11] P. Promvonge, S. Sripattanapipat, S. Tamna, S. Kwankaomeng, C. Thianpong, Numerical investigation of laminar heat transfer in a square channel with 45° inclined baffles, *International Communications in Heat and Mass Transfer* 37 (2010) 170-177.

[12] Kumar, R.P. Saini, J.S. Saini, Effect of roughness width ratio in discrete multi v-shaped rib roughness on thermohydraulic performance of solar air heater, *Heat and Mass Transfer* 51 (2015) 209-220.

[13] Lanjewar, J.L. Bhagoria, R.M. Sarviya, Heat transfer and friction in solar air heater duct with W-shaped rib roughness on absorber plate, *Energy* 36 (2011) 4531-4541.

[14] P. Promvonge, W. Changcharoen, S. Kwankaomeng, C. Thianpong, Numerical heat transfer study of turbulent square-duct flow through inline V-shaped discrete ribs, *International Communication Heat and Mass Transfer* 38 (2011) 1392-1399.

[15] S.K. Saini, R.P. Saini, Development of correlations for Nusselt number and friction factor for solar air heater with roughened duct having arc-shaped wire as artificial roughness, *Solar Energy* 82 (2008) 1118-1130.

[16] Y.H. Huang, C.H. Chen, Y.H. Liu, Nonboiling heat transfer and friction of air/water mist flow in a square duct with orthogonal ribs, *Journal of Thermal Science and Engineering Applications* 9 (2017) 041014.

[17] S. Sripattanapipat, P. Promvonge, Numerical analysis of laminar heat transfer in a channel with diamond-shaped baffles, *International Communication Heat and Mass Transfer* 36 (2009) 32-38.

[18] Thianpong, T. Chompookham, S. Skullong, P. Promvonge, Thermal characterization of turbulent flow in a channel with isosceles triangular ribs, *International Communication Heat and Mass Transfer* 36 (2009) 712-717.

[19] P. Sriromreun, C. Thianpong, P. Promvonge, Experimental and numerical study on heat transfer enhancement in a channel with Z-shaped baffles, *International Communication Heat and Mass Transfer* 39 (2012) 945-952.

[20] P. Promvonge, C. Thianpong, Thermal performance assessment of turbulent channel flow over different shaped ribs, *International Communication Heat and Mass Transfer* 35 (2008) 1327-1334.

[21] S. Skullong, S. Kwankaomeng, C. Thianpong, P. Promvonge, Thermal performance of turbulent flow in a solar air heater channel with rib-groove turbulators, *International Communication Heat and Mass Transfer* 50 (2014) 34-43.

[22] L. Wang, B. Sunden, Experimental investigation of local heat transfer in a square duct with various-shaped ribs, *Heat and Mass Transfer* 43 (2007) 759-766.

[23] M.M. Sahu, J.L. Bhagoria, Augmentation of heat transfer coefficient by using 90° broken transverse ribs on absorber plate of solar air heater, *Renewable Energy* 30 (2005) 2057-2063.

[24] K.R. Aharwal, B.K. Gandhi, J.S. Saini, Experimental investigation on heat transfer enhancement due to a gap in an inclined continuous rib arrangement in a rectangular duct of solar air heater, *Renewable Energy* 33 (2008) 585-596.

[25] M.E. Taslim, T. Li, D.M. Kercher, Experimental heat transfer and friction in channels roughened with angled, V-shaped, and discrete ribs on two opposite walls, *Journal of Turbomachinery* 118 (1996) 20-28.

[26] S. Singh, B. Singh, V.S. Hans, R.S. Gill, CFD investigation on Nusselt number and friction factor of solar air heater duct roughened with non-uniform cross-section transverse rib, *Energy* 84 (2015) 509-517.

[27] P.R. Chandra, C.R. Alexander, J.C. Han, Heat transfer and friction behaviour in rectangular channels with varying number of ribbed walls, *International Journal of Heat and Mass Transfer* 46 (2003) 481-495.

[28] P. Promvonge, S. Skullong, S. Kwankaomeng, C. Thianpong, Heat transfer in square duct fitted diagonally with angle-finned tape—Part 1: experimental study, *International Communication Heat and Mass Transfer* 39 (2012a) 617-624.

[29] P. Promvonge, S. Skullong, S. Kwankaomeng, C. Thianpong, Heat transfer in square duct fitted diagonally with angle-finned tape-Part 2: numerical study, *International Communication Heat and Mass Transfer* 39 (2012b) 625-633.
[30] W. Yang, S. Xue, Y. He, W. Li, Experimental study on the heat transfer characteristics of high blockage ribs channel, *Experimental Thermal and Fluid Science* 83 (2017) 248-259.
[31] Z. Ke, C.L. Chen, K. Li, S. Wang, C.H. Chen, Vortex dynamics and heat transfer of longitudinal vortex generators in a rectangular channel, *International Journal of Heat and Mass Transfer* 132 (2019) 871-885.
[32] Y. Menni, A. Azzi, C. Zidani, Computational analysis of turbulent forced convection in a channel with staggered corrugated baffles, *Communications in Science and Technology* 16 (2016) 34-43.
[33] H. Benzenine, R. Saim, S. Abboudi, O. Imine, Numerical analysis of a turbulent flow in a channel provided with transversal waved baffles, *Thermal Science* 17 (2013) 801-812.
[34] R. Kumar, P. Chand, Performance enhancement of solar air heater using herringbone corrugated fins, *Energy* 127 (2017) 271-279.
[35] I. Azevedo, M. Lebouche, R. Devienne, Laminar cooling of pseudoplastic fluids flowing through cylindrical horizontal pipes, *International Journal of Heat and Fluid Flow* 16 (1995) 125–130.
[36] L.C. Demartini, H.A. Vielmo, S.V. Möller, Numeric and experimental analysis of the turbulent flow through a channel with baffle plates, *Journal of the Brazilian Society of Mechanical Sciences and Engineering* 26(2) (2004) 153-160.
[37] S. Skullong, C. Thianpong, P. Promvonge, Effects of rib size and arrangement on forced convective heat transfer in a solar air heater channel, *Heat and Mass Transfer* 51 (2015) 1475-1485.

ORCID iD

Houari Ameur https://orcid.org/0000-0003-2087-7574